DOI: 10.1002/chem.201000092

Iron-Catalyzed Halogenation of Alkanes: Modeling of Nonheme Halogenases by Experiment and DFT Calculations

Peter Comba* and Steffen Wunderlich[a]

Abstract: When the dichloroiron(II) complex of the tetradentate bispidine ligand L = 3,7-dimethyl-9-oxo-2,4-bis(2-pyridyl)-3,7-diazabicyclo[3.3.1]nonane-1,5-dicarboxylate methyl ester is oxidized with H_2O_2, *t*BuOOH, or iodosylbenzene, the high-valent Fe=O complex efficiently oxidizes and halogenates cyclohexane. Kinetic D isotope effects and the preference for the abstraction of tertiary over secondary carbon-bound hydrogen atoms (quantified in the halogenation of adamantane) indicate that C–H activation is the rate-determining step. The efficiencies (yields in stoichiometric and turnover numbers in catalytic reactions), product ratios (alcohol vs. bromo- vs. chloroalkane), and kinetic isotope effects depend on the oxidant. These results suggest different pathways with different oxidants, and these may include iron(IV)– and iron(V)–oxo complexes as well as oxygen-based radicals.

Keywords: density functional calculations · enzyme models · halogenation · iron · oxidation

Introduction

Iron-catalyzed biological halogenation occurs with heme haloperoxidases and the recently discovered and characterized α-ketoglutarate-dependent nonheme halogenases (αKGH).[1–4] While chloroperoxidases generate a metal-bound hypochlorite ion which is capable of halogenating electron-rich organic substrates, the αKG-dependent nonheme Fe^{II} halogenases can also halogenate the less reactive electron-poor alkanes. The enzyme SyrB2 catalyzes the chlorination of L-threonine, a key step in the synthesis of the fungicide syringomycin E,[3] and recent studies on halogenases revealed the existence of high-spin Fe^{IV}=O centers as reactive intermediates.[5,6] These are proposed to be generated from Fe^{II} and molecular dioxygen, and believed to abstract a hydrogen atom from the substrate. In a "rebound step", similar to that known from heme- and non-heme-catalyzed hydroxylation reactions, a halogen atom is then thought to be transferred from the Fe^{III} center to the substrate radical. The structurally related αKG-dependent oxygenases, for example, the thoroughly studied taurine dioxygenase (TauD), lead in an analogous reaction sequence to hydroxylated products.[7,8] Given the similarity of the active sites and relevant intermediates, it is conceivable that the radical intermediate competes in the "rebound" step with the Fe^{III}OH and Fe^{III}Cl sites. However, until recently[9] all attempts to detect alcohol products in halogenases failed.[3] A number of alternative explanations for the observed halogenation chemoselectivity have been discussed: 1) The relative reactivities may be related to the redox potentials of the "rebound sites", which increase in the order $Br^{\bullet} < Cl^{\bullet} < OH^{\bullet}$ ($Br^{\bullet} + e^- \rightarrow Br^-$, 1.07 V vs. SHE; $Cl^{\bullet} + e^- \rightarrow Cl^-$, 1.36 V; $OH^{\bullet} + e^- \rightarrow OH^-$, 2.02 V).[10] 2) The selectivity is a result of the hydrogen-bonding pattern at the active site.[11] 3) The enzyme selectivity is due to the positioning of the substrate.[3] 4) The selectivity may be influenced by differing dynamics in the "rebound intermediate".[5] 5) In two recent computational studies the halogenation selectivity was proposed to be due to deactivation of the "OH rebound site" by either CO_2, formed in the halogenation cycle (decarboxylation of the α-ketoglutarate cofactor),[12] or by protonation of the hydroxyl group.[13] A thorough experimental study on SyrB2 indicates that substrate positioning is a major reason for enzyme selectivity.[9]

Biotic[1] and abiotic[14] iron-catalyzed halogenation reactions of alkanes attract increasing attention in environmental sciences because, among others, volatile alkyl halides are known to lead to the depletion of the stratospheric ozone layer.[14] We assume that abiotic natural production of halogenated hydrocarbon compounds may involve high-valent

[a] Prof. Dr. P. Comba, S. Wunderlich
Universität Heidelberg
Anorganisch-Chemisches Institut , INF 270
69120 Heidelberg (Germany)
Fax: (+49) 6221-546617
E-mail: peter.comba@aci.uni-heidelberg.de

Supporting information for this article is available on the WWW under http://dx.doi.org/10.1002/chem.201000092.

iron compounds, and it is of interest to fully understand these processes. So far there are no low-molecular weight biomimetic complexes which have been shown to catalytically halogenate alkanes, and which would allow a thorough study of possible mechanistic pathways for enzymatic and environmentally important reactions. Also, most of the reasons for the chemoselectivity given above are not relevant for simple coordination compounds, and any observed selectivity in model systems may help to resolve the still-disputed selectivity issue. Moreover, biomimetic halogenation catalysts could instigate the development of promising new catalysts for selective halogenation of substrates of industrial interest.[15]

Stoichiometric halogen atom transfer from $[Fe^{III}(tpa)(X)_2]$ (tpa = tris[(2-pyridyl)methyl]amine) to cyclohexane with *tert*-butyl hydroperoxide (TBHP) as oxidant has been reported.[10] Based on product distribution and selectivity a Gif-type process[16] was excluded, and this was supported by a recent computational study, which proposes, similar to the related hydroxylation, an $[Fe^{V}{=}O(tpa)(Cl)]^{2+}$ species (OH replaced by Cl) as the key reactive intermediate.[11] That is, similar to the enzymatic reactions, alkane hydroxylation and halogenation are proposed to follow analogous pathways but, in contrast to the enzymes, the tpa-based biomimetic systems are proposed to involve $Fe^{V}{=}O$ instead of $Fe^{IV}{=}O$ active sites.

Here, we report an experimental and DFT computational study on the catalytic halogenation (Cl or Br) of cyclohexane with the highly active iron(II) complex of the tetradentate bispidine ligand L (L = 3,7-dimethyl-9-oxo-2,4-bis(2-pyridyl)-3,7-diazabicyclo[3.3.1]nonane-1,5-dicarboxylate methyl ester)[17–21] and H_2O_2, TBHP or iodosylbenzene (PhIO) as external oxidant. Questions addressed and discussed in this study are 1) how efficient and selective is iron/bispidine-based halogenation of alkanes?, 2) which types of high-valent intermediates are of importance, that is, 3) what are the mechanistic pathways? (that generally assumed is shown in Scheme 1); specifically, whether a substrate radical intermediate is formed, how stable it is, and how selective the halogenation is compared to hydroxylation (studied previously with our iron–bispidine systems[19,22]), whether the bispidine-based model reaction is mechanistically related to biotic and/or abiotic natural processes, and whether an efficient and selective catalytic process can be developed with this type of catalyst.

Results and Discussion

The iron(II) bispidine complex $[Fe^{II}(L)Cl_2]$ transforms cyclohexane with a stoichiometric amount of TBHP as oxidant quantitatively to an approximately 1:1 mixture of chloro- or bromocyclohexane and cyclohexanol (see Table 1). With stoichiometric amounts of H_2O_2 or PhIO as oxidant, the overall yields are much lower (22 and 7%, respectively) but the chlorination reactions are selective. The yield of chlorocyclohexane increases to 40% when an excess of PhIO (ten-fold) is used and the reaction time is increased to 24 h. Catalytic reactions with an excess of a chloride salt in the reaction mixtures yield up to five turnovers (TON) of the chlorinated product, with PhIO chlorocyclohexane is produced selectively, while TBHP and H_2O_2 produce mixtures with different amounts of halocyclohexane and cyclohexanol (see Table 1). Interestingly and not unexpectedly, this system, which has been shown before to be an efficient biomimetic catalyst for the epoxidation/*cis*-dihydroxylation of alkenes[18] and for the hydroxylation of alkanes,[19] and which is known to form high-valent iron species of various constitution and electronic configuration,[18,19] with a ferryl complex of unprecedented oxidation power,[23] unambiguously catalyzes the halogenation of alkanes and, given that a high-valent oxidant is formed (see below), is the first functional halogenase model system, albeit not an efficient one.

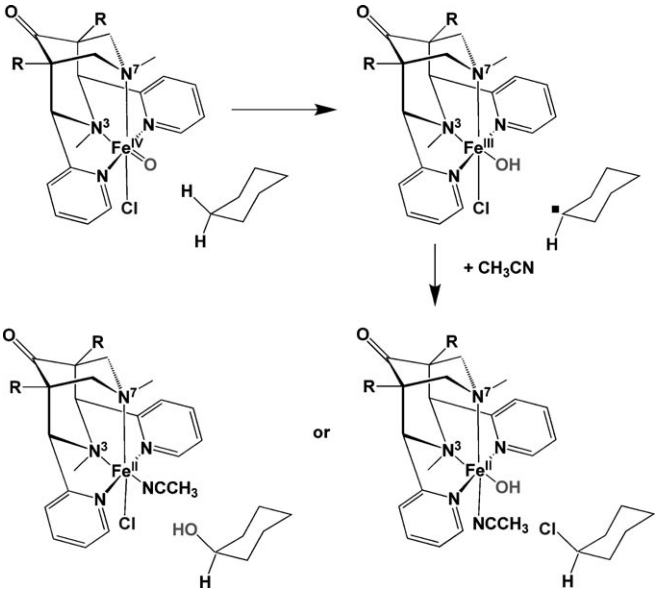

Scheme 1. Proposed mechanism for the chlorination of cyclohexane by $[Fe^{IV}{=}O(L)Cl]^{+}$ (R = CO_2CH_3; only the more stable of the two possible isomers is shown, $Fe^{IV}{=}O$ *trans* to N3).

Table 1. Results of the stoichiometric (% yield) and catalytic (TON) oxidation reactions of cyclohexane (standard deviations in parentheses).

X	Oxidant	$C_6H_{11}X$	$C_6H_{11}OH$	$C_6H_{10}O$
Cl	TBHP[a]	44.3(13)%	52.9(15)%	2.4(1)%
Br	TBHP[a]	43.4(38)%	54.9(24)%	0.3(1)%
Cl	TBHP[b]	5.1(1) TON	55.4(32) TON	0.1(1) TON
Br	TBHP[b]	1.6(1) TON	56.1(2) TON	0.4(1) TON
Cl	H_2O_2[a]	19.2(32)%	1.9(4)%	0.5(2)%
Cl	H_2O_2[b]	0.3(1) TON	0.5(1) TON	0.5(1) TON
Cl	PhIO[a]	6.9(14)%	0.2(1)%	0.2(1)%
Cl	PhIO (10 equiv, 35 min)[a]	17.0(11)%	0.1(1)%	0.1(1)%
Cl	PhIO (10 equiv, 24 h)[a]	39.9(12)%	0.1(1)%	0.1(1)%
Cl	PhIO (24 h)[b]	3.7(3) TON	0.0(0) TON	0.2(1) TON

[a] Stoichiometric reaction : 700 mM substrate (C_6H_{12} + Bu_4NX)/7 mM oxidant/7 mM iron complex; 35 min, CH_3CN (abs), 298 K, argon (unless otherwise specified). [b] Catalytic reaction: 700 mM substrate (C_6H_{12} + Bu_4NX)/70 mM oxidant/0.7 mM catalyst, otherwise identical conditions as above.

Whereas $[Fe^{IV}{=}O(L)(NCCH_3)]^{2+}$ shows, as expected for an $S=1$ ferryl complex, an absorption in the electronic spectrum at 760 nm with $\varepsilon = 130\,L\,mol^{-1}\,cm^{-1}$, this disappears when Cl^- is added to the solution (formation of a chloro complex; a similar effect is observed when H_2O is added to a solution of the ferryl complex in MeCN). However, the solution of the chloro complex is shown to oxidize substrates like ferrocene to the ferrocenium cation nearly quantitative yield (80%, see the Supporting Information). This is a strong indication for a reactive ferryl complex, and high-spin ($S=2$) electronic configuration is expected for the hydroxo and chloro complexes on the basis of the spectrochemical series. Indeed, a high-spin configuration was predicted by DFT for electronic reasons (peudo-Jahn–Teller distortion),[24] and the oxo hydroxo complex was shown by DFT (in agreement with the corresponding experimental data) to be the catalytically active oxidant in the oxidation of alkenes[18] and alkanes.[19]

Interestingly, in the hydroxylation of cyclohexane with the $[Fe^{IV}{=}O(L)(NCCH_3)]^{2+}$ catalyst, significant differences in product distributions were observed in dependence on the oxidant (PhIO vs. H_2O_2), and this was attributed to the possibility of two parallel reaction channels, involving $Fe^{IV}{=}O$ and $Fe^{V}{=}O$.[19] This interpretation was supported by DFT, and it was also shown computationally that $[Fe^{V}{=}O(L)(OH)]^{2+}$ is accessible (albeit less easily)[25] and highly reactive.[19] Thus, for the halogenation reactions discussed here (see Table 1), pathways based on high-spin $Fe^{IV}{=}O$ and $Fe^{V}{=}O$ may need to be taken into account (note that the SyrB2 biosystem involves a high-spin $Fe^{IV}{=}O$ intermediate,[5,6] and an $Fe^{V}{=}O$-based mechanism has been proposed for the stoichiometric reaction with the tpa-based complex[10,11]). While a high-spin $Fe^{IV}{=}O$ complex (five-coordinate, not very reactive)[26] and an $Fe^{V}{=}O$ complex[27] have been fully characterized, so far we have not been able to trap and spectroscopically unambiguously characterize our putative high-spin iron(IV) and iron(V) complexes. However, the significant differences in the halogenation reactions in terms of yield and chemoselectivity (see Table 1) suggest that different reaction channels might operate. It is known that the reaction of the iron(II) complexes with PhIO exclusively yields reactive ferryl intermediates, and these have been thoroughly characterized for iron bispidine complexes with pentadentate derivatives of L,[28–30] which have low-spin ($S=1$) electronic configuration, and this also is observed for $[Fe^{IV}{=}O(L)(NCCH_3)]^{2+}$.[23]

The reaction of the iron(II) bispidine complex of L with TBHP was studied in detail.[31] The end-on *tert*-butylperoxo complex $[Fe^{III}(OO\mathit{t}Bu)(L)(X)]^{n+}$ (X = NCMe, BF_4^-), generated from the Fe^{II} precursor and TBHP in MeCN, has an electronic transition at 605 nm. When the analogous iron(II) chloro complex is treated with TBHP, a similar absorption is observed (580 nm; see the Supporting Information). As a consequence of homolytic cleavage of the peroxide bond, alkoxy radicals are produced from Fe^{III}–OO*t*Bu systems together with the ferryl complexes. In our system, this therefore might lead to radical side reactions with a loss of selectivity in the oxidation reactions (Scheme 2).[32]

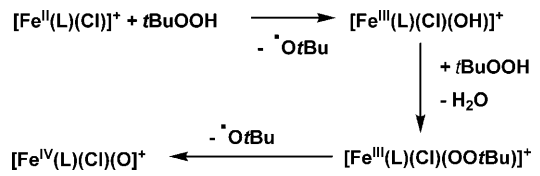

Scheme 2. Proposed mechanism for the formation of $[Fe^{IV}{=}O(L)(Cl)]^+$ from the iron(II) precursor and TBHP as oxidant.

Oxidation of the iron(II) bispidine complex of L with H_2O_2 was thoroughly analyzed by DFT calculations.[25] The preferred pathway is direct oxidation to $[Fe^{IV}(OH)_2(L)]^{2+}$, a precursor of $[Fe^{IV}{=}O(OH_2)(L)]^{2+}$. However, other channels to $[Fe^{IV}{=}O(OH_2)(L)]^{2+}$ and $[Fe^{V}{=}O(OH_2)(L)]^{3+}$ are also feasible,[25] and this may result in a variety of oxidants and reaction channels for the reaction with cyclohexane. Since radical-based processes reduce the selectivity, it appears that $Fe^{IV}{=}O$ (as in the reaction with PhIO) and possibly also $Fe^{V}{=}O$ lead to selective halogenation.

Kinetic deuterium isotope effects (KIEs) were determined for the three stoichiometric chlorination reactions with PhIO, TBHP, and H_2O_2 as oxidants by using 1:3 mixtures of cyclohexane and $[D_{12}]$cyclohexane as substrate, followed by analysis of the ratio of the halogenated products ($C_6H_{11}X$ vs. $C_6D_{11}X$). The observed primary KIEs of 14, 9, and 3 for PhIO, TBHP and H_2O_2, respectively, are significant and reveal that hydrogen abstraction is the rate-determining step of the halogenation reaction. The differences in the KIE values are a further indication for different reaction channels for each oxidant (see above), that is, depending on the oxidant, there are various possible reactive species (oxo Fe^{IV}, oxo Fe^{V}, O-based radicals), and the formation of each of those may also depend on the oxidant used. A very large primary KIE has been reported for the halogenases,[5,9] and the largest (but significantly smaller) KIE in our systems is observed with PhIO. The significantly lower KIE with H_2O_2 could be due to OH radicals (KIE between 1 and 2)[33,34] and/or an $Fe^{V}{=}O$-based pathway (support for the latter suggestion comes from the DFT-based analysis, see below).

The preferential abstraction of tertiary over secondary hydrogen atoms from adamantane as substrate ($\{[C^3]/[C^2]\}\times 3$) was investigated to qualitatively analyze the presence and stability (lifetime) of alkyl radicals. The values of 33, 8.6, 2.1 for PhIO, TBHP and H_2O_2, respectively, are as expected in the same order as the KIEs and indicate a significant lifetime of the alkyl radical intermediate. This is also supported by an experiment in which bromocyclohexane is formed from $[Fe^{IV}{=}O(L)(Cl)]^{2+}$ in the presence of CH_2Br_2.[35]

The chemoselectivity was also studied with PhIO as oxidant in a mixed Br/Cl system, specifically also to analyze the influence of the oxidation potentials of the coordinated hydroxide/chloride/bromide (see Introduction).[10] When a 1:1 mixture of $[Fe(L)(Br)_2]$ and $[Fe(L)(Cl)_2]$ is treated with one equivalent of PhIO, selective formation of bromocyclohexane is observed. This may be due to relative differences

in the first or second transition-state energies (formation or decay of the radical intermediate). If the first transition state were responsible for the selectivity, significantly different KIEs for chlorination and bromination would be expected. These were therefore measured, and are 14 and 9 for chlorination and bromination, respectively. These are values which we consider to be too similar to each other to explain the observed selectivity. Moreover, similar energies were obtained by DFT for the first transition states of the chlorination and bromination reactions ($\Delta G^{\neq} = 51.9\,kJ\,mol^{-1}$ for $[Fe^{IV}{=}O(L)(Cl)]^+$, $\Delta G^{\neq} = 58.4\,kJ\,mol^{-1}$ for $[Fe^{IV}{=}O(L)(Br)]^+$, see below). We therefore attribute the selectivity to the differing reactivity of the radical intermediate. This is also supported by the fact that the corresponding fluorination reaction of cyclohexane is not observed.[36]

Density functional calculations were performed to investigate the two probable reaction channels with the bispidine complexes of $XFe^{IV}{=}O$ and $XFe^{V}{=}O$ (X = Cl, Br) as reactive intermediates for the halogenation and hydroxylation of cyclohexane. There are two possible isomers each, with the oxo group *trans* to N3 or N7 (Scheme 1 shows the more stable isomer with $Fe^{IV}{=}O$ *trans* to N3). All possible spin surfaces were considered, and selected structural parameters as well as energies of the relevant species are assembled in Table 2. Figure 1 shows the computed free-energy diagram for cyclohexane chlorination and hydroxylation by $[Fe^{IV}{=}O(L)(Cl)]^+$ with the more stable isomer (Fe–O *trans* to N3); the energy diagrams for the other isomer and for the corresponding bromination reactions are given as Supporting Information. As expected,[19,22,24] the two isomers of the ferryl oxidant and the corresponding transition states are similar in energy (see Table 2). However, consistent with all other experimental and computational data available for this system, the isomer with O *trans* to N3 is slightly more stable and more reactive than that with O *trans* to N7;[18,21,24,37] also, the high-spin electronic configuration is more stabilized

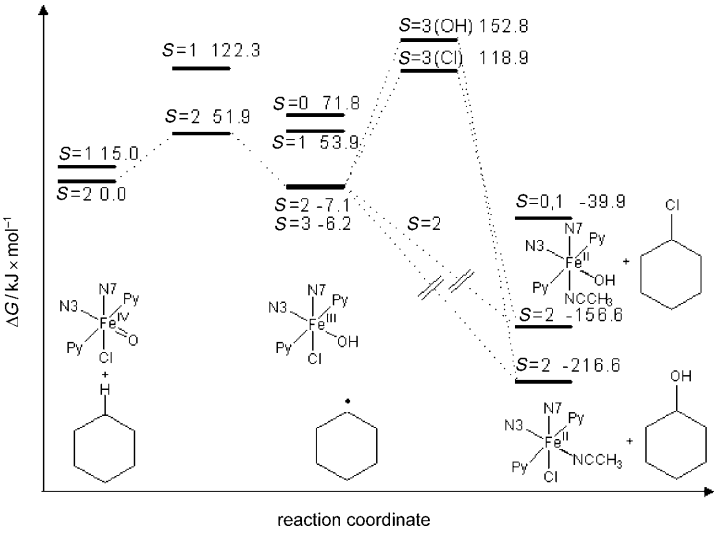

Figure 1. Free energy diagram for cyclohexane chlorination and hydroxylation by $[Fe^{IV}{=}O(L)(Cl)]^+$ (FeO *trans* to N3).

with respect to the triplet state in the geometry with O *trans* to N3, and this has some impact on the reactivity.[24]

The chloro ferryl complex $[Fe^{IV}{=}O(L)(Cl)]^+$ has a high-spin electronic configuration ($S=2$; the $S=1$ excited state is at 15.0 kJ mol^{-1}), an Fe–O distance of 1.64 Å and a rather long Fe–Cl bond of 2.39 Å.[38,39] An $S=2$ ground state was also reported for the non-heme iron halogenases[5,6] and, in fact, is the generally observed electronic configuration for enzymatic non-heme iron ferryl species.[40] For the model system discussed here, it is in agreement with earlier predictions[18,24] and with the expected relatively small ligand field due to the preference of the bispidine ligands for relatively large metal ions,[41,42] and expectations based on the small in-plane ligand field exerted by Cl^-, and this results altogether in a relatively low lying $d_{x^2-y^2}$-type orbital.

Hydrogen abstraction has an activation barrier of 51.9 kJ mol^{-1} and is the rate-limiting step; this is in agreement with the experimental data (KIEs, see above). The optimized structures of the first transition states for the halogenation and hydroxylation reactions on the quintet potential-energy surface (PES) with Fe–O *trans* to N3 and *trans* to N7 are shown in Figure 2. These transition state structures (high-spin $[(L)(Cl)Fe^{IV}{=}O{\cdots}H{\cdots}C_{substrate}]^{2+}$) correspond to early transition states with a C···H distance of 1.21 Å and an O···H distance of 1.39 Å for the *trans*-to-N3 structure. In the course of the reaction, the spin

Table 2. Calculated geometric parameters for the two isomers of $[Fe^{IV}{=}O(L)(X)]^+$ and their energetic parameters in cyclohexane halogenation.[a]

	$[Fe^{IV}{=}O(L)(Cl)]^+$				$[Fe^{IV}{=}O(L)(Br)]^+$			
O *trans* to	N3		N7		N3		N7	
spin *S*	1	2	1	2	1	2	1	2
Fe–N3	2.12	2.15	2.05	2.24	2.13	2.16	2.05	2.24
Fe–N7	2.23	2.39	2.39	2.32	2.25	2.39	2.40	2.33
Fe–py1	1.97	2.09	1.99	2.13	1.98	2.09	2.00	2.15
Fe–py2	1.97	2.09	1.99	2.13	1.98	2.09	2.00	2.15
Fe–O	1.65	1.64	1.64	1.64	1.65	1.64	1.64	1.65
Fe–X	2.34	2.39	2.32	2.33	2.50	2.57	2.48	2.50
N3-Fe-N7	85.9	82.6	83.8	82.3	85.6	82.4	83.5	82.1
py1-Fe-py2	162.4	159.1	167.6	154.6	162.8	158.8	166.8	153.9
O-Fe-X	90.5	91.9	91.9	91.9	88.9	89.7	90.5	90.0
N7-Fe-X	179.8	178.9	91.1	93.1	178.5	179.4	92.4	94.7
$\langle S^2 \rangle$	2.029	6.069	2.024	6.075	2.038	6.078	2.029	6.083
$\Delta G_{Fe^{IV}O}$[b]	15.0	0.0	17.6	5.9	14.0	0.0	26.4	9.7
$\Delta G^{\neq}$	122.3	51.9	128.5	63.5	119.1	58.4	40.4	72.2
$\Delta G_{halogenation}$		−156.6		−128.9		−144.1		−116.3
$\Delta G_{hydroxylation}$		−216.6		−195.6				

[a] Distances in Å, angles in degrees, energies in kJ mol^{-1}. [b] All energies quoted refer to the lowest lying isomer of the reactant, which was set as the origin.

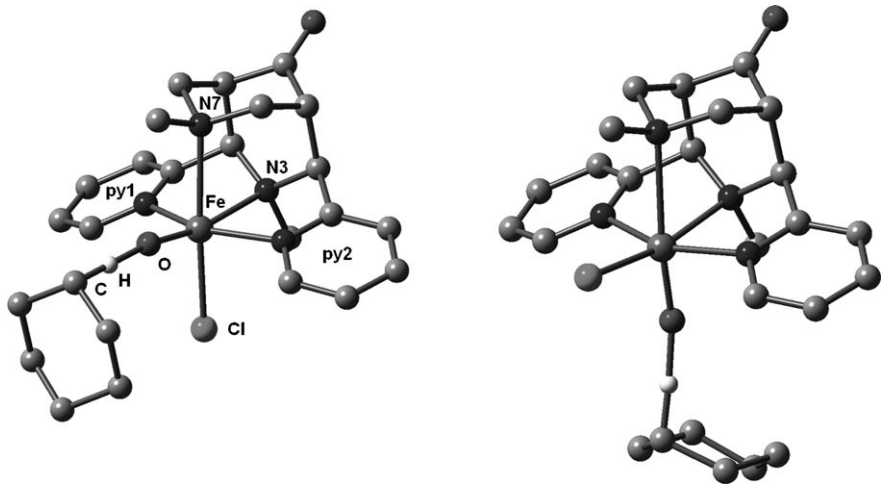

Figure 2. Structure of the transition state $[Fe^{IV}=O(L)Cl]^{+}\cdots C_6H_{12}$ along the quintet potential-energy surface (left: FeO *trans* to N3; right: FeO *trans* to N7).

density on C increases from −0.32 (transition state) to −0.89 for the high-spin Fe^{III} radical intermediate. The negative spin density on iron, which already develops at the transition state, suggests antiferromagnetic coupling and a preference for the $S=2$ over the $S=3$ spin state of the radical intermediate. Formation of chlorocyclohexane and cyclohexanol from the radical intermediate in its $S=2$ ground state is computed to be a barrierless process; this was carefully checked by relaxed scans on the PES for all reactions (O *trans* to N3 or N7, rebound to OH, Cl, or Br). Importantly, at a rather long distance between the carbon-based radical and the $Fe^{III}X$ site in the radical intermediate (the Supporting Information shows a plot of a PES scan of $Fe^{III}OH$ *trans* to N7 reacting with the cyclohexyl radical), there is good separation of the spin density (−1.0 at the carbon atom), that is, there is no self-interaction problem.[43] At smaller distances, electron transfer takes place to a radical cation, and this decays in a barrierless reaction. The same profile was obtained when solvation (MeCN) was taken into account.[45] A barrierless decay of the radical intermediate is in disagreement with the clear definition of this structure as a minimum on the PES and, more importantly, disagrees with the experimental data, whereby the $\{[C^3]/[C^2]\}\times 3$ values suggest a significant lifetime of the radical intermediate, and this is also supported by the selectivity for the halogenation pathway. A second transition state was localized on the $S=3$ spin surface (see Figure 1), but ferromagnetic coupling does not seem to be realistic (see above), and the computed energy barrier is too large to accommodate the observed experimental KIE values. The optimized structures of the second transition states on the $S=3$ surface were taken to analyze the influence of the entropy ($T\Delta S$) along the reaction coordinate shown in Figure 1, because this contribution is not included in a relaxed scan on the PES. Starting from the oxo Fe^{IV} reactant, $T\Delta S$ increases to 37.8 kJ mol^{-1} for the first transition state, decreases to 33.7 kJ mol^{-1} for the radical intermediate, and then rises to 48.0 and 46.6 kJ mol^{-1} for the hydroxylation and chlorination rebound states, respectively. The small differences in the contribution of $T\Delta S$ (48 vs. 47 kJ mol^{-1}) can therefore not explain the chemoselectivity. It is conceivable that the radical intermediate decays with a barrier for electron transfer from coordinated OH^-, Cl^-, or Br^-, respectively, to iron(III) on the $S=2$ spin surface, which is lower than that for hydrogen abstraction. This is in agreement with the observation that C–H activation is the rate-determining step, with the observed selectivity, and with the fact that we were able to optimize the structure of the radical intermediate in its $S=2$ ground state.

Cyclohexane oxidation catalyzed by $[Fe^{V}=O(L)(Cl)]^{2+}$ was also analyzed by DFT. The formation of the $Fe^{V}=O$ complex is a consequence of heterolytic cleavage of the O–O bond of the $Fe^{III}OOH$ precursor (when using H_2O_2; there is a corresponding process with TBHP), and this is known to be less favorable than formation of $Fe^{IV}=O$ but an alternative.[25] The $[Fe^{V}=O(L)(Cl)]^{2+}$ intermediate has a high-spin electronic configuration ($S=3/2$) with the low-spin ($S=1/2$) excited state at 44.5 kJ mol^{-1} (see Supporting Information, Table S1).[46] Once the $Fe^{V}=O$ species is formed, the halogenation reaction ($\Delta G=-386.9$ kJ mol^{-1}) is a barrierless process (relaxed scans on the PES), that is, hydrogen abstraction is barrierless and a radical intermediate was not found to be a minimum on the PES. Such a reaction would lead to a selectivity for halogenation, because after hydrogen abstraction the lone pair of the coordinated halide and not that of the hydroxo oxygen atom is pointing toward the singly occupied molecular orbital of the cyclohexyl radical, and the PES therefore directly leads to the halogenated alkane.[11] The experimentally observed KIEs suggest in general that the hydrogen abstraction step is rate-determining. This together with other experimental data discussed in detail above is at variance with a pure $Fe^{V}=O$-based pathway. However, the significantly lower KIEs and the lower $\{[C^3]/[C^2]\}\times 3$ values for adamantane with H_2O_2 as oxidant are consistent with two (or more) reaction channels, where one might be the nearly barrierless reaction due to an $Fe^{V}=O$ active site. Moreover, an Fe^{V}-based reaction has been discussed as a reasonable alternative in the Fe/L/cyclohexane system.[19]

Conclusion

The non-heme iron bispidine complex $[Fe^{II}(L)Cl_2]$, with H_2O_2, TBHP, or PhIO as external oxidant, is able to catalytically oxidize and halogenate cyclohexane and therefore is a

functional halogenase model, the first reported so far. The yield and selectivity strongly depend on the oxidant and reaction conditions. Generally, the selectivity for halogenation over hydroxylation is high, and OR radicals (R = *t*Bu in TBHP, H in H_2O_2) probably are responsible for the reduced selectivity in the TBHP-based reactions and the catalytic (but not the stoichiometric) reaction with H_2O_2. The stoichiometric reactions afford up to quantitative yield; therefore, pathways for catalyst deactivation must exist. The fact that the systems presented here are so far rather poor catalyst systems probably is largely due to the fact that ligand exchange to reproduce the halogeno iron(II) precatalysts is too inefficient. Thus, there are possibilities to optimize and considerably improve these systems. Interestingly, it appears that the least efficient process, that is, that with PhIO as oxidant, is the simplest reaction, probably involving only an XFe^{IV}=O-based pathway, and it selectively produces halogenated products. The yield with H_2O_2 is considerably higher, and the experimentally determined KIEs and computational data suggest that pathways based on XFe^{IV}=O and XFe^{V}=O may be involved. The high selectivity in the stoichiometric reaction was expected on the basis of the proposed direct oxidation of $[Fe^{II}(L)X_2]^{n+}$ with H_2O_2 to Fe^{IV}=O, which does not involve Fe^{III} intermediates and OH radicals.[18,25] The yield with TBHP as oxidant is nearly quantitative in stoichiometric reactions but this process is OR-radical-based and unselective.

A variety of proposals were made for the chemoselectivity of the enzyme-catalyzed reaction. From our results presented here it appears that both XFe^{IV}=O- and XFe^{V}=O-based processes should generally have high halogenation selectivity, and it emerges that decreasing selectivities are generally indicative of radical-based side reactions. The total selectivity required by biological reactions seems to be accomplished by enzyme-based substrate positioning,[9] an approach which is not available for simple low molecular weight compounds. The design of more efficient catalyst systems needs to prevent oxygen-based radicals and requires efficient ligand-exchange processes to produce high enough concentrations of the iron(II) halogenide precatalyst, and these are requirements which might be possible to meet.

Experimental Section

General: Chemicals (Aldrich, Fluka) and solvents were of highest possible grade and used as purchased. Mass spectra: Bruker ApexQe hybrid 9.4 FT-ICR or Finnigan TSW 700. Elemental analyses were performed by the analytical laboratories of the chemical institutes of the University of Heidelberg. Products were analyzed by GC on a Varian 3900 instrument with a ZB-1701 column.

Synthesis of the ligand and Fe bispidine complexes. Bispidine ligand L was synthesized as reported.[47] For the synthesis of the Fe^{II} chloro and bromo complexes, a suspension of 8.77 g (20.0 mmol) ligand L in acetonitrile (60 mL) was mixed with an equimolar amount of $FeCl_2$ or $FeBr_2$ under argon and strictly H_2O free conditions. The product started to precipitate after few minutes and, after stirring for 30 min at ambient temperature, was isolated in good yields by filtration, washed with cold MeCN (10 mL), and dried.[21] $[Fe(L)(Cl)_2]\cdot CH_3CN$: 85% yield, orange solid. ESI-MS (MeCN): *m/z*: 529.09438 $[Fe(L)(Cl)]^+$; elemental analysis (%) found: C 49.45, H 4.83, N 11.48; calcd for $C_{25}H_{29}Cl_2FeN_5O_5$ (M_r 606.28): C 49.53, H 4.82, N 11.55. $[Fe(L)Br_2]\cdot CH_3CN$: 82% yield, orange solid. ESI-MS (MeCN): *m/z*: 575.04158 $[Fe(L)(Br)]^+$; elemental analysis (%) found: C 43.12, H 4.22, N 10.04; calcd for $C_{25}H_{29}Br_2FeN_5O_5$ (M_r 695.18): C 43.19, H 4.20, N 10.07. $[Fe(L)F_2]\cdot 2.5\,H_2O$: $(Bu_4N)F$ (0.54 g2.07 mmol) was added to $[Fe(L)(NCCH_3)](OTf)_2$ in acetonitrile (0.60 g, 0.72 mmol). A red solid was obtained by filtration after 10 min at ambient temperature, washed with cold MeCN, and dried (yield of 93%). ESI-MS (MeCN): *m/z*: 513.1235 $[Fe(L)(F)]^+$; elemental analysis (%) found: C 47.96, H 5.46, N 9.66; calcd for $C_{46}H_{62}F_4Fe_2N_8O_{15}$ (M_r 1154.71): C 47.85, H 5.41, N 9.77.[21]

Stoichiometric oxidation of cyclohexane: In a typical reaction, 0.7 M cyclohexane was treated with 7 mM complex and 7 mM oxidant in MeCN (25 °C, Ar, H_2O-free). For the reactions with H_2O_2 and TBHP the oxidant was diluted to 0.3 mL and added by syringe pump over 30 min at 25 °C to a solution of the substrate and catalyst. The solution was stirred for a further 5 min after addition of the oxidant was completed. For the reaction with PhIO, the oxidant was added as a solid, and the reaction time was increased to 24 h (see Table 1). The product solution was absorbed onto a silica gel column and washed with MeCN (5 mL). Naphthalene was added as internal standard and the mixture was analyzed by GC. The retention times for the product peaks were compared with those of standard compounds and their identity was confirmed by GC-MS. All reactions were done in triplicate; the reported data is the average of these reactions.

Catalytic oxidation of cyclohexane: These reactions were conducted with concentrations of 0.7 mM catalyst, 70 mM oxidant, and 0.7 M substrate (cyclohexane and Bu_4NCl or Bu_4NBr) under the same conditions as for the stoichiometric experiments. The reaction was quenched by the addition of an equal volume of water, and the products were isolated by extraction with 3×2 mL Et_2O. The ether layers were combined, dried over anhydrous Na_2SO_4, and analyzed by GC.

Oxidation of adamantane: Identical conditions to those for stoichiometric cyclohexane oxidation were used but with final concentrations of 0.7 mM catalyst, 7 mM oxidant, and 7 mM substrate.

Determination of the KIEs: Identical conditions to those for stoichiometric cyclohexane oxidation were used but with a 1:3 mixture of cyclohexane (175 mM) and $[D_{12}]$cyclohexane (525 mM) followed by analysis of the product distribution of the halogenated alkane.

Computational studies: All DFT calculations were performed with the Jaguar 6.5 program package, unless otherwise specified[48] The B3LYP functional[49–51] and LACVP basis set (double ζ with a Los Alamos effective core potential for the Fe center and 6-31G for the other atoms) were used.[52,53] All intermediates were confirmed by frequency calculations with Gaussian 03.[54] Single-point calculations were performed on the B3LYP/LACVP optimized geometries by using the LACV3P++** basis set (LanL2DZ on the Fe center and 6-311++G** on the other atoms). The energies reported are those calculated at the B3LYP/LACV3P++** level and include zero point and free energy corrections, derived from the B3LYP/LACVP calculations. A simplified model system was used in all calculations, in which the ester groups on the ligand backbone were replaced by hydrogen atoms.

Acknowledgements

Financial support by the German Science Foundation (DFG Research Group FOR 763 "Natural Halogenation Processes") is gratefully acknowledged.

[1] F. H. Vaillancourt, E. Yeh, D. A. Vosburg, S. Garneau-Tsodikova, C. T. Walsh, *Chem. Rev.* **2006**, *106*, 3364.
[2] F. H. Vaillancourt, E. Yeh, D. A. Vosburg, S. E. O'Conner, C. T. Walsh, *Nature* **2005**, *436*, 1191.

[3] L. C. Blasiak, F. H. Vaillancourt, C. T. Walsh, C. L. Drewman, *Nature* **2006**, *440*, 368.
[4] F. H. Vaillancourt, J. Yin, C. T. Walsh, *Proc. Natl. Acad. Sci. USA* **2005**, *102*, 10111.
[5] D. P. Galonic, E. W. Barr, C. T. Walsh, J. M. Bollinger, Jr., C. Krebs, *Nat. Chem. Biol.* **2007**, *3*, 113.
[6] D. Galonic Fujimori, E. W. Barr, M. L. Matthews, G. M. Koch, J. R. Yonce, C. T. Walsh, J. M. Bollinger, Jr., C. Krebs, P. J. Riggs-Gelasco, *J. Am. Chem. Soc.* **2007**, *129*, 13408.
[7] J. C. Price, E. W. Barr, B. Tirupati, J. M. Bollinger, Jr., C. Krebs, *Biochemistry* **2003**, *42*, 7497.
[8] L. M. Hoffart, E. W. Barr, R. B. Guyer, J. M. Bollinger, Jr., C. Krebs, *Proc. Natl. Acad. Sci. USA* **2006**, *103*, 14738.
[9] M. L. Matthews, C. S. Neumann, L. A. Miles, T. L. Grove, S. J. Booker, C. Krebs, C. T. Walsh, J. M. Bollinger, Jr., *Proc. Natl. Acad. Sci. USA* **2009**, *106*, 17723.
[10] T. Kojima, R. A. Leising, S. Yan, L. Que, Jr., *J. Am. Chem. Soc.* **1993**, *115*, 11328.
[11] H. Noack, P. E. M. Siegbahn, *J. Biol. Inorg. Chem.* **2007**, *12*, 1151.
[12] S. P. de Visser, R. Latifi, *J. Phys. Chem. B* **2009**, *113*, 12.
[13] S. Pandian, A. M. Vincent, I. H. Hillier, N. A. Burton, *Dalton Trans.* **2009**, 6201.
[14] R. von Glasow, P. J. Crutzen in *Treatise on Geochemistry, Vol. 4*, Elsevier, Amsterdam, **2003**, p. 21.
[15] K.-H. van Pee in *Enzyme Catalysis in Organic Synthesis, Vol. 3*, 2nd ed., **2002**, p. 1267.
[16] D. H. R. Barton, D. Doller, *Acc. Chem. Res.* **1992**, *25*, 504.
[17] P. Comba, M. Kerscher, W. Schiek, *Prog. Inorg. Chem.* **2007**, *55*, 613.
[18] J. Bautz, P. Comba, C. Lopez de Laorden, M. Menzel, G. Rajaraman, *Angew. Chem.* **2007**, *119*, 8213; *Angew. Chem. Int. Ed.* **2007**, *46*, 8067.
[19] P. Comba, M. Maurer, P. Vadivelu, *J. Phys. Chem. A* **2008**, *112*, 13028.
[20] P. Comba, B. Nuber, A. Ramlow, *J. Chem. Soc. Dalton Trans.* **1997**, 347.
[21] H. Börzel, P. Comba, K. S. Hagen, M. Merz, Y. D. Lampeka, A. Lienke, G. Linti, H. Pritzkow, L. V. Tsymbal, *Inorg. Chim. Acta* **2002**, *337*, 407.
[22] P. Comba, M. Maurer, P. Vadivelu, *Inorg. Chem.* **2009**, *48*, 10389.
[23] P. Comba, S. Fukuzumi, H. Kotani, S. Wunderlich, *Angew. Chem.* **2010**, *122*, 2679; *Angew. Chem. Int. Ed.* **2010**, *49,* 2622.
[24] A. Anastasi, P. Comba, J. McGrady, A. Lienke, H. Rohwer, *Inorg. Chem.* **2007**, *46*, 6420.
[25] P. Comba, G. Rajaraman, H. Rohwer, *Inorg. Chem.* **2007**, *46*, 3826.
[26] J. England, M. Martinho, E. R. Farquhar, J. R. Frisch, E. L. Bominaar, E. Münck, L. Que, Jr., *Angew. Chem.* **2009**, *121*, 3676; *Angew. Chem. Int. Ed.* **2009**, *48*, 3622.
[27] F. Tiago de Oliveira, A. Chanda, D. Banerjee, X. Shan, S. Mondal, L. Que, Jr., E. L. Bominaar, E. Münck, T. J. Collins, *Science* **2007**, *315*, 835.
[28] M. R. Bukowski, P. Comba, C. Limberg, M. Merz, L. Que, Jr., T. Wistuba, *Angew. Chem.* **2004**, *116*, 1303; *Angew. Chem. Int. Ed.* **2004**, *43*, 1283.
[29] M. R. Bukowski, P. Comba, A. Lienke, C. Limberg, C. Lopez de Laorden, R. Mas-Balleste, M. Merz, L. Que, Jr., *Angew. Chem.* **2006**, *118*, 3524; *Angew. Chem. Int. Ed.* **2006**, *45*, 3446.
[30] J. Bautz, M. Bukowski, M. Kerscher, A. Stubna, P. Comba, A. Lienke, E. Münck, L. Que, Jr., *Angew. Chem.* **2006**, *118*, 5810; *Angew. Chem. Int. Ed.* **2006**, *45*, 5681.
[31] J. Bautz, P. Comba, L. Que, Jr., *Inorg. Chem.* **2006**, *45*, 7077.
[32] P. A. MacFaul, K. U. Ingold, D. D. M. Wayner, L. Que, Jr., *J. Am. Chem. Soc.* **1997**, *119*, 10594.
[33] G. V. Buxton, C. L. Greenstock, W. P. Helman, A. B. Ross, *J. Phys. Chem. Ref. Data Monogr.* **1988**, 513.
[34] D. T. Sawyer, C. Kang, A. Llobet, C. Redman, *J. Am. Chem. Soc.* **1993**, *115*, 5817.
[35] CH_2Br_2 (100 equiv, 700 mM) was added to a solution for a stoichiometric reaction under otherwise usual conditions (see Experimental Section).
[36] In an experiment on the fluorination of cyclohexane under stoichiometric conditions with $[Fe(L)F_2]$ and all three oxidants (PhIO, H_2O_2,and TBHP), no formation of $C_6H_{11}F$ was observed. This is not surprising because the oxidation potential of fluoride (2.87 V vs. SHE) is significantly higher than that of OH^- (2.02 V, see above).
[37] P. Comba, J. Lefebvre, J. Madhavan, S. Wunderlich, unpublished results.
[38] The quality of the theoretical method used (see Experimental Section) and of the data produced (see Table 2 and the table with the corresponding data for the Fe^V-based pathway in the Supporting Information) were validated by additional calculations with a larger basis set: structural data and energetics similar to those given in the tables were obtained with Ahlrich's TZVP basis set (optimization with Gaussian 03 (see ref. [54]).
[39] A. Schäfer, C. Huber, R. Ahlrichs, *J. Chem. Phys.* **1994**, *100*, 5829.
[40] W. Nam, *Acc. Chem. Res.* **2007**, *40*, 465.
[41] P. Comba, M. Kerscher, M. Merz, V. Müller, H. Pritzkow, R. Remenyi, W. Schiek, Y. Xiong, *Chem. Eur. J.* **2002**, *8*, 5750.
[42] C. Bleiholder, H. Börzel, P. Comba, R. Ferrari, A. Heydt, M. Kerscher, S. Kuwata, G. Laurenczy, G. A. Lawrance, A. Lienke, B. Martin, M. Merz, B. Nuber, H. Pritzkow, *Inorg. Chem.* **2005**, *44*, 8145.
[43] A. J. Johansson, M. R. A. Blomberg, E. M. Siegbahn, *J. Phys. Chem. C* **2007**, *111*, 12397.
[44] *Handbook of Chemistry and Physics*, CRC Press, Boca Raton, **1985**–**1986**.
[45] Solvation by MeCN was calculated with the self-consistent reaction field (SCRF) method implemented in Jaguar and with a dielectric constant of 36.64.[44]
[46] Note that the $S=^1/_2$ state is highly spin contaminated ($\langle S^2\rangle = 1.66$).
[47] R. Haller, U. Ashauer, *Arch. Pharm.* **1985**, *318*, 405.
[48] JAGUAR 6.5 ed., Schrödinger, Schrödinger LLC, New York, **2005**.
[49] A. D. Becke, *J. Chem. Phys.* **1992**, *96*, 2155.
[50] A. D. Becke, *J. Chem. Phys.* **1992**, *97*, 9173.
[51] A. D. Becke, *J. Chem. Phys.* **1993**, *98*, 5648.
[52] J. P. Hay, W. R. Wadt, *J. Chem. Phys.* **1985**, *82*, 99.
[53] R. A. Friesner, R. B. Murphy, M. D. Beachy, M. N. Ringlanda, W. T. Pollard, B. D. Dunietz, Y. X. Cao, *J. Phys. Chem. A* **1999**, *103*, 1913.
[54] Gaussian 03, Revision B.03, M. J. Frisch, G. W. Trucks, H. B. Schlegel, G. E. Scuseria, M. A. Robb, J. R. Cheeseman, J. A. Montgomery, Jr., T. Vreven, K. N. Kudin, J. C. Burant, J. M. Millam, S. S. Iyengar, J. Tomasi, V. Barone, B. Mennucci, M. Cossi, G. Scalmani, N. Rega, G. A. Petersson, H. Nakatsuji, M. Hada, M. Ehara, K. Toyota, R. Fukuda, J. Hasegawa, M. Ishida, T. Nakajima, Y. Honda, O. Kitao, H. Nakai, M. Klene, X. Li, J. E. Knox, H. P. Hratchian, J. B. Cross, V. Bakken, C. Adamo, J. Jaramillo, R. Gomperts, R. E. Stratmann, O. Yazyev, A. Austin, R. Cammi, C. Pomelli, J. W. Ochterski, P. Y. Ayala, K. Morokuma, G. A. Voth, P. Salvador, J. J. Dannenberg, V. G. Zakrzewski, S. Dapprich, A. D. Daniels, M. C. Strain, O. Farkas, D. K. Malick, A. D. Rabuck, K. Raghavachari, J. B. Foresman, J. V. Ortiz, Q. Cui, A. G. Baboul, S. Clifford, J. Cioslowski, B. B. Stefanov, G. Liu, A. Liashenko, P. Piskorz, I. Komaromi, R. L. Martin, D. J. Fox, T. Keith, M. A. Al-Laham, C. Y. Peng, A. Nanayakkara, M. Challacombe, P. M. W. Gill, B. Johnson, W. Chen, M. W. Wong, C. Gonzalez, J. A. Pople, Gaussian Inc., Wallingford, CT, **2003**.

Received: January 14, 2010
Published online: May 10, 2010

